Guanidinium-induced denaturation by breaking of salt bridges

Meuzelaar, H.; Panman, M.R.; Woutersen, S.

Protein Folding

Guanidinium-Induced Denaturation by Breaking of Salt Bridges

Heleen Meuzelaar, Matthijs R. Panman, and Sander Woutersen*

Abstract: *Despite its wide use as a denaturant, the mechanism by which guanidinium (Gdm$^+$) induces protein unfolding remains largely unclear. Herein, we show evidence that Gdm$^+$ can induce denaturation by disrupting salt bridges that stabilize the folded conformation. We study the Gdm$^+$-induced denaturation of a series of peptides containing Arg/Glu and Lys/Glu salt bridges that either stabilize or destabilize the folded conformation. The peptides containing stabilizing salt bridges are found to be denatured much more efficiently by Gdm$^+$ than the peptides containing destabilizing salt bridges. Complementary 2D-infrared measurements suggest a denaturation mechanism in which Gdm$^+$ binds to side-chain carboxylate groups involved in salt bridges.*

Guanidinium chloride is a widely used denaturant, but despite extensive investigations[1–20] the mechanism of its denaturing effect is still largely unknown. Different mechanisms have been proposed, involving direct effects in which guanidinium (Gdm$^+$) interacts with specific parts of a protein,[5,6,8,11,13,17] indirect effects (Gdm$^+$-induced perturbation of the hydrogen-bonding network of water),[7,16,21] and combined direct and indirect effects.[18] Recent experiments have shown that Gdm$^+$ interacts weakly with water,[22,23] suggesting that Gdm$^+$ denaturation occurs mainly through a direct mechanism. Many studies indicate a preferential interaction of Gdm$^+$ with specific amino-acid side chains.[5,6,12,14,24,25] In particular, small-angle neutron scattering and molecular dynamics (MD) simulations suggest that Gdm$^+$ stacks against aromatic[5,11] and aliphatic[5] side chains, thereby reducing hydrophobic contributions to protein stability.[20] On the other hand, MD simulations also show that Gdm$^+$ can perturb electrostatic interactions by interacting with negatively charged side groups.[6] The potential role of such electrostatic interactions in Gdm$^+$-induced denaturation is demonstrated by the different Gdm$^+$ sensitivities of coiled-coil peptides with similar hydrophobic packings but different electrostatic interactions.[1] Finally, experimental[15] and MD[5,15,24] work shows that Gdm$^+$ has an affinity for the Gdm$^+$ moiety of arginine side groups, resulting from stacking interactions. The question therefore arises if and how Gdm$^+$ denaturation might involve disruption of salt bridges (electrostatic interactions between oppositely charged amino acid side chains), which play an essential role in the conformational stability of many proteins. Although MD simulations have shown evidence that Gdm$^+$ binds to COO$^-$ groups

forming salt bridges,[6,26,27] a systematic study of this effect is still lacking. Herein, we investigate the denaturation by Gdm$^+$ of specifically tailored α-helical peptides containing different types of stabilizing or destabilizing salt bridges.

The investigated peptide sequences are listed in Table 1, together with their abbreviated names which indicate the distance and order of the salt-bridge forming residues.

Table 1: Sequences of the investigated peptides (Ac = acetyl, A = Ala, E = Glu, R = Arg, K = Lys).

Sequence	Abbreviation
Ac-A(EAAAR)$_3$A-NH$_2$	$(i+4)$ER
Ac-A(ARAAE)$_3$A-NH$_2$	$(i+3)$RE
Ac-A(EAAAK)$_3$A-NH$_2$	$(i+4)$EK
Ac-A(AKAAE)$_3$A-NH$_2$	$(i+3)$KE

Depending on the spacing and order of the oppositely charged residues, they can form salt bridges that stabilize or destabilize the folded state:[28,29] the salt bridges in the $(i+4)$ER and $(i+4)$EK peptides stabilize the folded conformation, whereas the salt bridges in the $(i+3)$RE and $(i+3)$KE peptides stabilize the unfolded conformation.[28] We use Cl$^-$ as the counter ion of Gdm$^+$, as it is known to have little effect on its denaturing efficiency, as opposed to other counter ions such as sulfate.[11,30–32] The Na$^+$ counter ions of the peptide are present in concentrations that are negligible compared to the Gdm$^+$ concentrations used.

Figure 1a shows CD spectra of peptide $(i+4)$ER (in which the α-helix is stabilized by E:R salt bridges) at increasing concentrations of Gdm$^+$ (see the Supporting Information for experimental details). In the absence of Gdm$^+$, the CD spectrum exhibits the two minima (at 208 and 222 nm) characteristic for α-helical structure. Addition of increasing amounts of Gdm$^+$ causes a gradual decrease in the CD signal, reflecting the unfolding of the α-helix. The denaturation profile (inset of Figure 1a) shows that even relatively low concentrations of Gdm$^+$ already reduce the α-helical population significantly, reflecting a strong sensitivity to the denaturant. Figure 1c shows the temperature dependence of the helix content for three different Gdm$^+$ concentrations. These unfolding curves (melting temperatures of $T_m = 312.9 \pm 1.2$ K (0 M Gdm$^+$), $T_m = 302.6 \pm 2.1$ K (0.4 M Gdm$^+$), and $T_m = 291.9 \pm 2.5$ K (1.5 M Gdm$^+$)) confirm that increasing levels of Gdm$^+$ reduce the stability of the folded state. Interestingly, the melting temperature at the highest Gdm$^+$ concentration is equal to the melting temperature of 295.7 ± 1.4 K observed for this peptide when its salt bridges are broken by protonating the Glu carboxylate groups.[33] These identical melting temperatures already hint at a denaturation mechanism in which Gdm$^+$ breaks the salt bridges.

[*] Dr. H. Meuzelaar, Dr. M. R. Panman, Prof. Dr. S. Woutersen
Van 't Hoff Institute for Molecular Sciences, University of Amsterdam
Science Park, 904, 1098 XH Amsterdam (The Netherlands)
E-mail: s.woutersen@uva.nl

Supporting information for this article is available on the WWW under http://dx.doi.org/10.1002/anie.201508601.
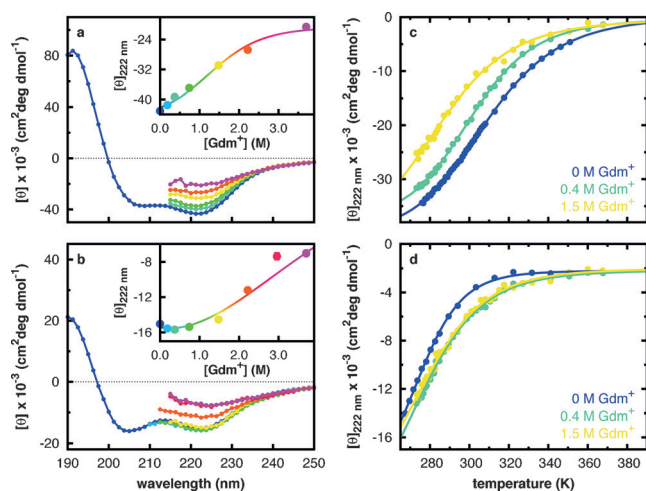
Figure 1. UV-CD Spectra (at increasing [Gdm$^+$]) of (a) peptide $(i+4)$ER and (b) peptide $(i+3)$RE. Owing to the absorption of Gdm$^+$ at short wavelengths, no CD data at wavelengths < 210 nm can be obtained. The insets show the ellipticity at 222 nm versus Gdm$^+$ concentration. The solid curves are a global least-squares fit to Equation (1). Thermal unfolding curves of (c) peptide $(i+4)$ER and (d) peptide $(i+3)$RE for different [Gdm$^+$]. The solid curves are a least-squares fit to a two-state model.[34]

Figure 1b and 1d show the UV–CD data of peptide $(i+3)$RE, in which the α-helix is destabilized by salt bridges (that is, the salt bridges can form only if the helix is unfolded).[28,29] Note that the ratio of the 208 and 222 nm minima varies between peptides, because the 208 nm minimum also contains contributions from unstructured states.[35] The Gdm$^+$-induced CD changes of peptide $(i+3)$RE indicate that the α-helix content remains the same with increasing Gdm$^+$ concentrations up to ≈1.5 M (Figure 1b). Adding modest concentrations of Gdm$^+$ even slightly increases the helical content (inset of Figure 1b). We confirm this small, but significant stabilization of the folded conformation upon adding Gdm$^+$ by measuring the melting temperatures, for which we find $T_m = 270.0 \pm 2.3$ K (0 M Gdm$^+$), $T_m = 275.9 \pm 1.0$ K (0.4 M Gdm$^+$), and $T_m = 276.3 \pm 1.0$ K (1.5 M Gdm$^+$). Further addition of Gdm$^+$ eventually causes denaturation of the α-helix. Comparison of the Gdm$^+$ denaturation curves of peptides $(i+3)$RE and $(i+4)$ER (insets of Figure 1a,b) shows that peptide $(i+3)$RE is considerably more resistant to Gdm$^+$ denaturation than $(i+4)$ER. The initial increase of the helical content suggests that Gdm$^+$ binds to the salt-bridging side groups of $(i+3)$RE, thereby inhibiting the formation of structure-destabilizing salt bridges and inducing a shift of the folding–unfolding equilibrium towards the folded, α-helical state. A further increase of the Gdm$^+$ concentration eventually results in denaturation, probably owing to binding of Gdm$^+$ to the remainder of the peptide. This latter effect counteracts the stabilizing effect caused by Gdm$^+$ inhibiting the destabilizing salt bridge, and at sufficiently high Gdm$^+$ concentration causes the peptide to unfold.

The different sensitivities to Gdm$^+$ of the peptides with helix-stabilizing and destabilizing Glu$^-$:Arg$^+$ salt bridges indicate that Gdm$^+$ causes denaturation by breaking salt bridges through interaction with one or both of the amino

acid side groups involved in the salt bridges. Gdm$^+$ may break the salt bridges by interacting with the carboxylate (COO$^-$) side groups of Glu,[1,6,14] but also by stacking with the Arg side chain.[5,15,24,36] To investigate which specific side chain, Glu$^-$ or Arg$^+$, determines the Gdm$^+$ sensitivity, we performed Gdm$^+$-induced unfolding measurements on similar peptides in which the Arg residues were replaced by Lys (to which Gdm$^+$ does not bind[15,24]). Figure 2a shows that Gdm$^+$ reduces the helix content of the salt bridge-optimized peptide $(i+4)$EK in the same manner as for the Arg-based peptide $(i+4)$ER. The
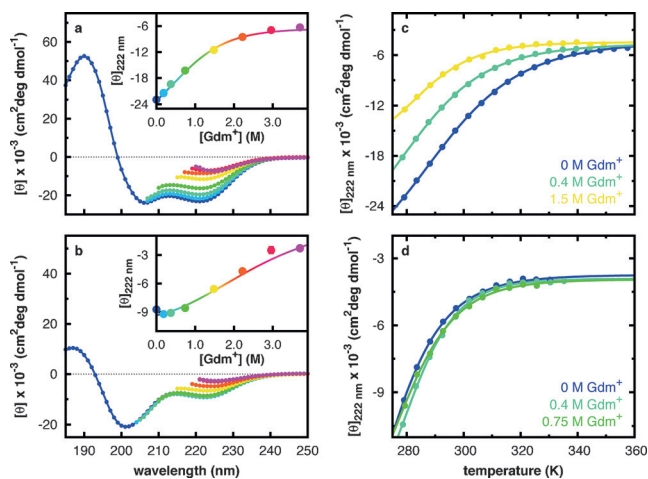

Figure 2. UV-CD Spectra (at increasing [Gdm$^+$]) of (a) peptide $(i+4)$EK (containing stabilizing salt bridges) and (b) peptide $(i+3)$KE (containing destabilizing salt bridges). The insets show the ellipticity at 222 nm versus Gdm$^+$ concentration. The solid curves are a global least-squares fit to Equation (1). Thermal unfolding curves of (c) peptide $(i+4)$EK and (d) peptide $(i+3)$KE for different [Gdm$^+$]. The solid curves are a least-squares fit to a two-state model.[34]

Gdm$^+$ denaturation curve of peptide $(i+4)$EK is also very similar to that of $(i+4)$ER (insets of Figure 2a and Figure 1a). We find $T_m = 292.6 \pm 0.7$ K (0 M Gdm$^+$), $T_m = 284.3 \pm 1.4$ K (0.4 M Gdm$^+$), and $T_m = 283.8 \pm 2.6$ K (1.5 M Gdm$^+$) (Figure 2c), confirming that Gdm$^+$ reduces the stability of the $(i+4)$EK peptide. The peptide $(i+3)$KE containing conformation-destabilizing Glu$^-$:Lys$^+$ salt bridges maintains its folded conformation up to Gdm$^+$ concentrations of 0.75 M (Figure 2b), indicating less denaturant activity of Gdm$^+$ as compared to $(i+4)$EK. Again, the functional shape of the Gdm$^+$ denaturation curve of the Lys-based peptide is similar to that of the Arg-containing variant (insets of Figures 2b and 1b). The melting temperatures of peptide $(i+3)$KE with increasing Gdm$^+$ concentration are $T_m = 274.8 \pm 1.5$ K (0 M Gdm$^+$), $T_m = 280.3 \pm 2.0$ K (0.4 M Gdm$^+$), and $T_m = 277.6 \pm 4.7$ K (0.75 M Gdm$^+$), showing that modest Gdm$^+$ concentrations enhance the fold stability of peptide $(i+3)$KE, probably by disrupting the unfavorable salt bridges. The similar effect of Gdm$^+$ on the Arg- and Lys-based peptides indicates that Gdm$^+$ interacts predominantly with the COO$^-$ side groups of Glu.

To date, the association of Gdm$^+$ with carboxylate groups in aqueous solution has only been studied indirectly, in

particular through the effect of association on the conductivity[37] or on the carboxylate pK_a.[34] To examine in a more direct manner if Gdm$^+$ binds to COO$^-$ groups, we performed 2D-IR spectroscopy on a deuterated aqueous solution of guanidine acetate (GdmDAc). We recently demonstrated that 2D-IR spectroscopy can be used to probe the formation and structure of salt bridges between Gdm$^+$ and Ac$^-$ in DMSO by detecting the vibrational coupling between the CN$_3$D$_6^+$-modes of Gdm$^+$ and the COO$^-$-stretch mode of Ac$^-$.[39] Here, we investigate if association of Gdm$^+$ and COO$^-$ in aqueous solution can be observed in a similar manner. Figure 3a presents the IR spectra of isolated Gdm$^+$ (GdmDCl, cyan) and Ac$^-$ (NaAc, purple). The spectrum of GdmD$^+$ shows a broad peak centered at 1600 cm^{-1}, arising from CN$_3$ antisymmetric stretch and ND$_2$ scissors motion.[39]
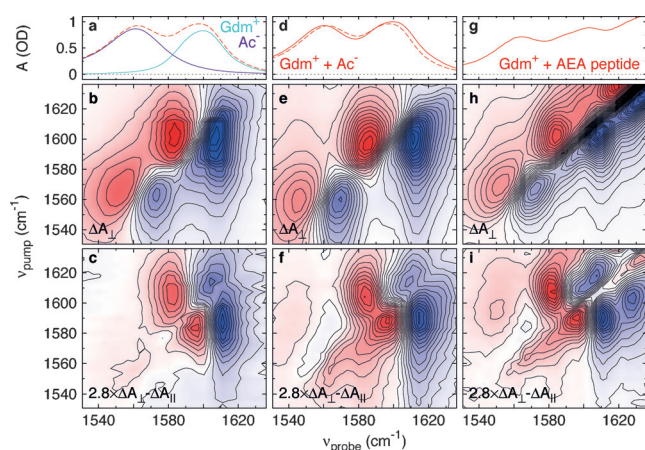
Figure 3. a) Normalized IR spectra of solutions of isolated Gdm$^+$ (GdmDCl) and Ac$^-$ (NaAc), both at 1.5 M concentration in D$_2$O (solvent subtracted). The dashed spectrum is the sum of the Gdm$^+$ (GdmDCl) and Ac$^-$ (NaAc) spectra. b) 2D-IR spectrum constructed by adding the 2D-IR spectra of isolated Gdm$^+$ and Ac$^-$. This is the spectrum expected if no interaction between Gdm$^+$ and Ac^{-1} would occur. Blue indicates negative absorption change, red positive absorption change. c) Polarization difference 2D-IR spectrum ($2.8\Delta A_\perp - \Delta A_\parallel$), constructed in the same manner as (b). d) Normalized IR spectrum of 1.5 M GdmAc solution in D$_2$O (solvent subtracted). e) 2D-IR spectrum of this solution. f) Polarization difference 2D-IR spectrum ($2.8\Delta A_\perp - \Delta A_\parallel$) of this solution. g) Normalized IR spectrum of 2 M Ac-Ala-Glu-Ala-NH$_2$ peptide + 2 M Gdm$^+$ solution in D$_2$O (solvent subtracted); the response above 1620 cm^{-1} is due to the amide modes in the peptide. h) 2D-IR and i) polarization difference 2D-IR spectrum ($2.8\Delta A_\perp - \Delta A_\parallel$) of this solution. All 2D-IR spectra were obtained with a pump–probe delay of 1 ps.

The frequency of the COO$^-$-antisymmetric-stretch mode of Ac$^-$ is 1560 cm^{-1}. Upon mixing equimolar NaAc and GdmDCl solutions, we observe frequency shifts of the infrared bands of Gdm$^+$ and Ac$^-$ (Figure 3d, where we compare the spectrum of GdmDAc to that constructed by adding the spectra of equimolar GdmDCl and NaAc solutions): the CN$_3$D$_6^+$ frequency of Gdm$^+$ increases by 2 cm^{-1}, while the COO$^-$-antisymmetric-stretch frequency decreases by 2 cm^{-1}. This increased frequency splitting between two vibrational modes suggests that the modes are coupled.[40] To confirm this, we performed 2D-IR measurements on deuter-

ated solutions of GdmDCl, NaAc, and GdmDAc (Figure 3). To compare the 2D-IR response of isolated Gdm$^+$ and Ac$^-$ ions with that of a solution containing Gdm$^+$:Ac$^-$ dimers, we constructed 2D-IR spectra of a (hypothetical) mixture of monomeric Gdm$^+$ and Ac$^-$ by adding the individual experimental 2D-IR responses of NaAc and GdmDCl solution (Figure 3b,c). The cross-peak pair at (ν_{probe}, ν_{pump}) = (1595, 1585) and (1585, 1605) cm^{-1} (positive parts), originating from the coupling between the two CN$_3$D$_6^+$ modes of Gdm$^+$,[39] is present in both Figure 3c and 3f. By contrast, the 2D-IR polarization-difference spectrum of the GdmDAc solution displays two more weak cross peaks between the CN$_3$D$_6^+$ and COO$^-$ modes (Figure 3e). These cross peaks overlap with the more intense diagonal peaks, and can be seen more clearly in the polarization-difference spectrum (Figure 3f).[39,41] The cross peaks, which indicate coupling between two vibrational modes, are positive–negative doublets in the ν_{probe} direction.[40] The Gdm$^+$/COO$^-$ cross-peak response at (ν_{probe}, ν_{pump}) ≈ (1540, 1585) and (1560, 1580), which is similar to that observed for Gdm$^+$:Ac$^-$ dimers in DMSO,[39] indicates that the CN$_3$D$_6^+$ modes of Gdm$^+$ are vibrationally coupled to the COO$^-$-stretch mode of Ac$^-$ owing to association of the two ions. The corresponding COO$^-$/Gdm$^+$ cross-peak response at (ν_{probe}, ν_{pump}) ≈ (1585, 1560) and (1615, 1560) overlaps with the much stronger Gdm$^+$/Gdm$^+$ cross peaks, but its presence can be seen by comparing Figure 3f and 3c. We observe these Gdm$^+$/COO$^-$ interactions only at relatively high concentrations, in agreement with the reported low Gdm$^+$:Ac$^-$ association constant.[38] To confirm that Gdm$^+$ also binds to peptide COO$^-$ groups, we investigated the peptide Ac-Ala-Glu-Ala-NH$_2$, the COO$^-$-containing segment of the α-helical peptide. The peptide is terminated with neutral end groups (acetyl on the N terminus, amide on the C terminus) to mimic the complete peptide as well as possible, and prevent effects of charged end groups. This peptide is sufficiently soluble to perform 2D-IR measurements (Figure 3h,i), in which we observe the same cross peaks as in the case of Gdm$^+$:Ac$^-$ dimer, confirming that the same type of Gdm$^+$:COO$^-$ binding occurs.

We can describe the denaturation data (insets of Figure 1a,b and Figure 2a,b) using a model that takes into account both the specific binding of Gdm$^+$ to the Glu COO$^-$ group (disrupting the salt bridges), and its weaker, non-specific binding to the remainder of the peptide. The effect of Gdm$^+$ on the folding equilibrium arises from the fact that it has different association constants for binding to the peptide in its folded and unfolded states.[42] The dependence of the free-energy change ΔG_{unf} of the folded→unfolded transition on the Gdm$^+$ concentration C is given by:[42]

$$\Delta G_{unf}(C) = \Delta G^0_{unf} - n_{sites} RT[\ln(1 + K_u C) - \ln(1 + K_f C)] - mC, \quad (1)$$

where ΔG^0_{unf} is the free energy of unfolding in absence of Gdm$^+$, $C = $ [Gdm$^+$], $n_{sites} = 3$ the number of binding sites (in this case Glu COO$^-$ groups[43]) in the peptide, R the gas constant, T the temperature, K_u and K_f the association constants for Gdm$^+$:Glu$^-$ binding in the unfolded and folded states respectively, and m a constant. The second term accounts for the specific binding of Gdm$^+$ to the Glu

carboxylate groups, the third term for the non-specific binding of Gdm$^+$.[34] The $(i+4)$ER and $(i+4)$EK peptides have salt bridges in the folded state, but not in the unfolded state. Therefore, for these peptides $K_u > K_f$ (since in the folded state the Glu$^-$:Arg$^+$ or Glu$^-$:Lys$^+$ salt bridges compete with Glu:Gdm$^+$ binding, whereas in the unfolded state this does not happen). The second and third terms in Equation (1) are therefore both negative so that ΔG_{unf} decreases (and the peptides start to unfold) even at the lowest Gdm$^+$ concentrations. In the $(i+3)$RE and $(i+3)$KE peptides on the other hand, salt bridges are present in the unfolded state but cannot be formed in the folded state, so that $K_f > K_u$ (since in the unfolded state, Glu$^-$:Gdm$^+$ binding has to compete with Glu$^-$:Arg$^+$ or Glu$^-$:Lys$^+$ salt-bridge formation), and the second term in Equation (1) is positive, leading to an increase of ΔG_{unf} with increasing [Gdm$^+$]. However, for sufficiently high Gdm$^+$ concentrations this increase is counter-acted by the weaker, non-specific binding of Gdm$^+$ to the peptide (represented by the third term), which dominates at high concentrations. This explains why, in the $(i+3)$RE and $(i+3)$KE peptides, the helical conformation is stabilized at low Gdm$^+$ concentration, but denatured at higher Gdm$^+$ concentration. We can describe our data by assuming that the Glu$^-$:Gdm$^+$ association constant in the absence of competing salt bridges (that is, K_u of peptides $(i+4)$ER and $(i+4)$EK, and K_f of peptides $(i+3)$RE and $(i+3)$ K) is equal to the association constant 0.37 M^{-1} of Gdm$^+$ and acetate.[38] The Gdm$^+$-carboxylate association constants in the presence of competing salt bridges are unknown, as are the values of m. These values are obtained from simultaneous least-squares fits to the $(i+4)$ER and $(i+3)$RE, and to the $(i+4)$EK and $(i+3)$KE peptides, respectively. The sets of Arg- and Lys-based peptides are treated independently, as the Gdm$^+$ association constant in the presence of competing salt bridges depends on whether these competing salt bridges are formed with Arg or with Lys. From the fits (shown as the curves in the insets of Figure 1 and Figure 2), we obtain for the association constants in presence of salt bridges 0.03 ± 0.02 M^{-1} for the Arg-based peptides, and 0.09 ± 0.03 M^{-1} for the Lys-based peptides. As expected, these values are much lower than the association constant in the absence of salt brides (0.37 M^{-1}).[38] The lower association constant in the presence of Glu$^-$:Arg$^+$ salt bridges as compared to Glu$^-$:Lys$^+$ salt bridges indicates that Glu$^-$:Arg$^+$ salt bridges are stronger (and so less easily broken up by Gdm$^+$) than Glu$^-$:Lys$^+$ salt bridges, in agreement with the lower melting temperature of the peptides containing the latter. For the parameter m characterizing the non-specific binding, we obtain 500 ± 40 and 530 ± 40 cal mol^{-1}M^{-1} for the Arg and Lys-based peptides; the similarity of the values confirms the non-specific character of the Gdm$^+$ binding described by the third term in Equation (1).

To conclude, our experiments show a correlation between the presence of structure-stabilizing salt bridges in a peptide and its sensitivity to Gdm$^+$ denaturation, and provide evidence that Gdm$^+$ can denature proteins by breaking salt bridges through competitive binding with COO$^-$ side groups. The [Gdm$^+$]-dependent behavior of peptides containing destabilizing salt bridges indicates that besides breaking the salt bridges, Gdm$^+$ also interacts with the remainder of the peptide, and that this interaction dominates at high Gdm$^+$ concentrations. The comparatively low Gdm$^+$:COO$^-$ association constant provides an explanation for the high Gdm$^+$ concentrations typically required for protein denaturation.

How to cite: *Angew. Chem. Int. Ed.* **2015**, *54*, 15255–15259
Angew. Chem. **2015**, *127*, 15470–15474

[1] O. D. Monera, C. M. Kay, R. S. Hodges, *Protein Sci.* **1994**, *3*, 1984–1991.
[2] J. S. Smith, J. M. Scholtz, *Biochemistry* **1996**, *35*, 7292–7297.
[3] C. E. Dempsey, T. J. Piggot, P. E. Mason, *Biochemistry* **2005**, *44*, 775–781.
[4] N. Shukla, A. N. Bhatt, A. Aliverti, G. Zanetti, V. Bhakuni, *FEBS J.* **2005**, *272*, 2216–2224.
[5] P. E. Mason, J. W. Brady, G. W. Neilson, C. E. Dempsey, *Biophys. J.* **2007**, *93*, L04–L06.
[6] E. P. O'Brien, R. I. Dima, B. Brooks, D. Thirumalai, *J. Am. Chem. Soc.* **2007**, *129*, 7346–7353.
[7] J. N. Scott, N. V. Nucci, J. M. Vanderkooi, *J. Phys. Chem. A* **2008**, *112*, 10939–10948.
[8] L. Guo, P. Chowdhury, J. M. Glasscock, F. Gai, *J. Mol. Biol.* **2008**, *384*, 1029–1036.
[9] S. J. Kim, B. Born, M. Havenith, M. Gruebele, *Angew. Chem. Int. Ed.* **2008**, *47*, 6486–6489; *Angew. Chem.* **2008**, *120*, 6586–6589.
[10] W. K. Lim, J. Rösgen, S. W. Englander, *Proc. Natl. Acad. Sci. USA* **2009**, *106*, 2595–2600.
[11] P. E. Mason, C. E. Dempsey, L. Vrbka, J. Heyda, J. W. Brady, P. Jungwirth, *J. Phys. Chem. B* **2009**, *113*, 3227–3234.
[12] P. E. Mason, C. E. Dempsey, G. W. Neilson, S. R. Kline, J. W. Brady, *J. Am. Chem. Soc.* **2009**, *131*, 16689–16696.
[13] C. E. Dempsey, P. E. Mason, P. Jungwirth, *J. Am. Chem. Soc.* **2011**, *133*, 7300–7303.
[14] J. Heyda, M. Kožíšek, L. Bednárova, G. Thompson, J. Konvalinka, J. Vondrášek, P. Jungwirth, *J. Phys. Chem. B* **2011**, *115*, 8910–8924.
[15] A. Kubíčková, T. Křížek, P. Coufal, E. Wernersson, J. Heyda, P. Jungwirth, *J. Phys. Chem. Lett.* **2011**, *2*, 1387–1389.
[16] I. M. Pazos, F. Gai, *J. Phys. Chem. B* **2012**, *116*, 12473–12478.
[17] A. Huerta-Viga, S. Woutersen, *J. Phys. Chem. Lett.* **2013**, *4*, 3397–3401.
[18] S. K. Jha, S. Marqusee, *Proc. Natl. Acad. Sci. USA* **2014**, *111*, 4856–4861.
[19] D. A. Turton, K. Wynne, *J. Phys. Chem. B* **2014**, *118*, 4600–4604.
[20] R. D. Macdonald, M. Khajehpour, *Biophys. Chem.* **2015**, *196-206*, 25–32.
[21] R. J. Cooper, S. Heiles, M. J. DiTucci, E. R. Williams, *J. Phys. Chem. A* **2014**, *118*, 5657–5666.
[22] P. Mason, G. Neilson, C. Dempsey, A. Barnes, J. Cruickshank, *Proc. Natl. Acad. Sci. USA* **2003**, *100*, 4557–4561.
[23] S. T. van der Post, K.-J. Tielrooij, J. Hunger, E. H. Backus, H. J. Bakker, *Faraday Discuss.* **2013**, *160*, 171–189.

[24] J. Vondrášek, P. E. Mason, J. Heyda, K. D. Collins, P. Jungwirth, *J. Phys. Chem. B* **2009**, *113*, 9041–9045.

[25] H. Hofmann, D. Nettels, B. Schuler, *J. Chem. Phys.* **2013**, *139*, 121930.

[26] J. Heyda, M. Kožíšek, L. Bednárova, G. Thompson, J. Konvalinka, J. Vondrášek, P. Jungwirth, *J. Phys. Chem. B* **2011**, *115*, 8910–8924.

[27] M. Mandal, C. Mukhopadhyay, *Phys. Chem. Chem. Phys.* **2014**, *16*, 21706–21716.

[28] S. Marqusee, R. L. Baldwin, *Proc. Natl. Acad. Sci. USA* **1987**, *84*, 8898–8902.

[29] B. M. P. Huyghues-Despointes, J. M. Scholtz, R. L. Baldwin, *Protein Sci.* **1993**, *2*, 80–85.

[30] C. E. Dempsey, P. E. Mason, J. W. Brady, G. W. Neilson, *J. Am. Chem. Soc.* **2007**, *129*, 15895–15902.

[31] C. E. Dempsey, P. E. Mason, P. Jungwirth, *J. Am. Chem. Soc.* **2011**, *133*, 7300–7303.

[32] E. Wernersson, J. Heyda, A. Kubíčková, T. Křížek, P. Coufal, P. Jungwirth, *J. Phys. Chem. B* **2010**, *114*, 11934–11941.

[33] H. Meuzelaar, M. Tros, A. Huerta-Viga, C. N. van Dijk, J. Vreede, S. Woutersen, *J. Phys. Chem. Lett.* **2014**, *5*, 900–904.

[34] T. E. Creighton, *Proteins: Structure and Molecular Properties*, 3rd ed., Freeman, New York, **2013**.

[35] R. F. Sommese, S. Sivaramakrishnan, R. L. Baldwin, J. A. Spudich, *Protein Sci.* **2010**, *19*, 2001–2005.

[36] K. T. No, K.-Y. Nam, H. A. Scheraga, *J. Am. Chem. Soc.* **1997**, *119*, 12917–12922.

[37] J. Hunger, R. Neueder, R. Buchner, A. Apelblat, *J. Phys. Chem. B* **2013**, *117*, 615–622.

[38] B. Springs, P. Haake, *Bioorg. Chem.* **1977**, *6*, 181–190.

[39] A. Huerta-Viga, S. R. Domingos, S. Amirjalayer, S. Woutersen, *Phys. Chem. Chem. Phys.* **2014**, *16*, 15784–15786.

[40] P. Hamm, M. Zanni, *Concepts and Methods of 2D Infrared Spectroscopy*, Cambridge University Press, Cambridge, **2011**.

[41] A. Huerta-Viga, S. Amirjalayer, S. R. Domingos, H. Meuzelaar, A. Rupenyan, S. Woutersen, *J. Chem. Phys.* **2015**, *142*, 212444.

[42] J. A. Schellman, *Q. Rev. Biophys.* **2005**, *38*, 351–361.

[43] Based on the similarity of the Glu/Arg and Glu/Lys results, we ignore the association of Gdm^+ with Arg. Binding of Gdm^+ to Arg would not change the equation, but would cause an increase in the effective association constant.